NOTICE CONCERNING COPYRIGHT RESTRICTIONS

Geothermal Exploration using Hyperspectral Analysis over Dixie and Fairview Valleys, Nevada

Amie Lamb[1], Chris Kratt[2], and [1]Wendy Calvin[1]

[1]Geological Sciences, and the Great Basin Center for Geothermal Research
University of Nevada-Reno, Reno NV, USA
[2]Desert Research Institute, Reno NV
amiekl@gmail.com

Keywords

Hyperspectral remote sensing, HyMap, hydrothermal mineralogy, Elevenmile Canyon, Dixie Meadows, Pirouette Mountain

ABSTRACT

Two hyperspectral data sets were acquired over Dixie Valley and several other smaller adjacent basins that totaled more than 1700 km^2 of coverage. Hyperspectral analysis permits rapid identification of geothermal indicators such as hydrothermal alteration minerals and evaporite deposits over large surface areas. The hyperspectral data were acquired at 3m spatial resolution with 125 channels across the visible-near infrared and short-wave infrared wavelength regions. Data were collected over the northern portion of the valley in 2002 as part of a program sponsored by Lawrence Livermore National Lab. Our analysis of the 2002 data focuses on areas that have not been previously mapped. The second data set was funded by the Department of the Navy Geothermal Program Office, and acquired in September of 2010. Mineral maps were provided by the data vendor for the area covered in 2010 and augmented by our own analysis.

The study area spans the southern portion of Dixie Valley and northern Fairview Valley, located in Churchill County, Nevada approximately 60 air kilometers northeast of Fallon. Eleven geothermal prospects have been identified by high temperatures in shallow temp gradient wells, hot springs, and fumaroles along the entire extent of Dixie Valley. The Dixie Valley Geothermal System is the hottest known system in Nevada with temperatures above 285˚C at 3 km depth and a 63 MW power plant in the northern part of the valley that has been operational for over 30 years. Dixie Meadows and Coyote Canyon prospects are in exploratory drilling stages with plans for powerplant construction by Ormat, Inc. and Terra-gen, respectively, each with a predicted 62 MW output. Stillwater and Salt Wells geothermal plants are also within 25 km to the west of our study areas, though the geothermal systems are not necessarily related to the Dixie Valley prospects.

Comparing the hyperspectral data with known areas of high heat flow and analysis from other data sets (shallow-temperature surveys and LiDAR) we identified three regions for initial detailed examination, Elevenmile Canyon, Pirouette Mountain and Fairview Peak. Hyperspectral mineral mapping indicated two additional areas of interest in La Plata Canyon and eastern Dixie Meadows. We identified areas with hydrothermal alteration including kaolinite, alunite, opal, chlorite, and gypsum.

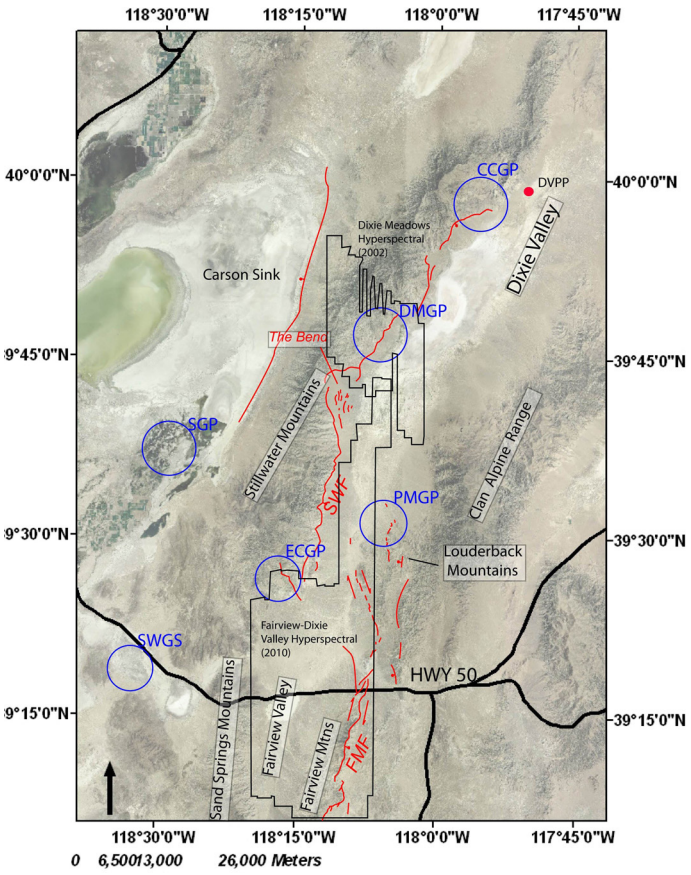

Figure 1. Study area with major features mapped. 1954 fault ruptures in red. Orange circles are hot springs, star is Dixie Town Center. Abbreviations: Geothermal systems (GS): CCGS – Coyote Canyon GS, DMGS – Dixie Meadows GS, DVPP –Dixie Valley Power Plant, ECGS - Elevenmile Canyon GS, PMGS – Pirouette Mountain; GS. Faults: FMF – Fairview Mountain Fault (oblique dextral normal); SWF – Stillwater Fault (normal).

Introduction

In 2010, the Navy Geothermal Program Office (NGPO) funded several exploration data sets that include: airborne hyperspectral remote sensing, LiDAR, shallow 2-m temperature probe surveys, and shallow temperature gradient drilling in southern Dixie Valley and Fairview Valley (DVFV). High temperatures in thermal gradient wells drilled in the early 1980s helped motivate NGPO to fund a phased, project scale exploration approach to DVFV. The geothermal prospects are poorly understood.

Numerous authors describe the use of hyperspectral remote sensing data sets for the identification of acid-sulfate mineral assemblages and chemical precipitates associated with both active and fossil geothermal systems (e.g. Kruse et al, 1999; Vaughan et al., 2005; Kratt et al., 2006 and 2010; and Littlefield et al., 2010). Regional to project scale areas can be quickly surveyed and analyzed to produce geothermal-indicator mineral maps that are associated with thermal fluid movement along structural features.

Hyperspectral mineral mapping results from the 2002 and 2010 data were validated in the field and laboratory spectral measurements. Selected X-ray diffraction analysis for more than 50 field samples will be conducted during the summer of 2011. In addition, field spectra were acquired along several transects. Our goals were to 1) recommend favorable areas for shallow temperature measurements; 2) combine our results with the LiDAR data for a more robust interpretation of favorable areas for thermal gradient drilling. Results for the LiDAR, temperature survey and drilling can be found, respectively, in Helton et al., Skord et al., and Lazaro et al., this issue.

Background

Local Geothermal Setting

Isotopic studies indicate that the Dixie Valley geothermal reservoir results from deep circulation in the highly fractured upper crust; magmatic thermal input is minor (Blackwell, 2007). During the past several decades workers have conducted dozens of studies, including geophysical, chemical, spectral, hydrological, and geological, to characterize the Dixie Valley geothermal system that supplies the Power Plant located in the northern portion of Dixie Valley. Data suggest that deeply circulating geothermal fluids hosted within Dixie Valley may generate all eleven recognized geothermal prospects spread along the extent of Dixie Valley (Blackwell, 2007).

Geological Setting

Northern Dixie Valley (DV) lies within an asymmetrical north-northeast trending alluvial-filled half-graben that dips to the west. Southern Dixie Valley is bound by active faults on both the east and west sides. DV is bound on the west by the Stillwater Range, and to the east by the Clan Alpine Range and Louderback Mountains (fig. 1). South of DV is Fairview Valley, which lies between Sand Springs Mountain to the west and Fairview Mountains to the east. Jurassic metamorphic sediments and volcanic units underlie Oligocene-Miocene volcanics, and are intruded by Jurassic gabbroic to Jurassic-Tertiary granitic intrusives (Willden and Speed, 1974). Southern Dixie and Fairview Valleys are aligned roughly north-south. South of Dixie Meadows, the strike of the Stillwater Mountains transitions from north-south to north-northeast at a feature descriptively named The Bend.

Extension in the area began in the middle Miocene, and resulted in one to two thousand meters of uplift of the Stillwater Range (John, 1995). Extension continues today as is evidenced by 1954 earthquakes (Caskey, 1996). Recent to Pleistocene faulting occurs on the east side of the mountain ranges in the study area. Faulting is normal in the Stillwater Mountains, and oblique in the Fairview Mountains. Elevenmile Canyon and Piroutte Mountain geothermal prospects occur in 1954 fault terminations (Mankhemthong et al., 2008). Faulds et al. (2006) identify fault terminations as favorable structural settings for geothermal systems. Dixie Meadows geothermal prospect is situated along a complicated fault termination.

Hydrothermal Indicators

Hydrothermal identifiers that can be mapped by hyperspectral remote sensing include siliceous sinter, tufa and minerals including opal, clays, hydrates, hydroxides, and iron oxides (Rowan et al., 2000).Hydrothermal minerals are commonly used as geothermometers (Reyes, 1990). The occurrence of hydrothermal minerals typical of geothermal systems depends on six factors: (a) temperature, (b), pressure, (c) rock type, (d) permeability, (e) fluid composition, and (f) duration of activity (Brown, 1978). Siliceous sinter precipitates from silica-saturated geothermal fluids in subaerial or sublacustrine environments, and indicates minimum temperatures of 180˚C (Renaut et al., 2002; Coolbaugh et al., 2010.) Hydrothermal alteration mineralogy due to thermal zonation has been documented by Bruhn et al. 2003) and is summarized in Table 1. Surface geothermal indicators include hotsprings and small fumaroles that are exposed in trenches.

Table 1. Summary of thermal zonation of hydrothermal alteration minerals (HAM). After Bruhn et al., 2003.

HAM Zone	Relative Depth	Dominant / Typical Minerals	Temp. Range (°C)	Typical Permeability
Argillic Zone	Shallowest	Montmorillonite ± (illite, chlorite, low-T zeolites)	<150-160	Extremely low – cap rock behavior
Illite-Chlorite Zone a.k.a Phyllitic Zone	Shallow	Mixed layer Illite-chlorite, high-T zeolite laumonite	Up to ≈ 200-250	Extremely low – cap rock behavior
Propylitic Zone	Deep	Ca-Al-silicates, epidote, 2ndary minerals ≈equlbrm w/NaCl waters e.g. adularia, albite, sulfides (e.g. pyrite, pyrrhotite, sphalerite); high-T zeolite is wairakite	Up to ≈ 300	Brittle behavior – high permeability pathway potential
Thermometamorphic (i.e. contact) Zone – *textural reorganization is prevalent*	Deepest	High-T mineral phases including amphiboles, pyroxenes, biotite, and garnets	Mineral formation temperatures range 700 and higher	Brittle behavior – high permeability pathway potential

Remote Sensing

It can be impossible to visually discern between some important temperature-variant hydrothermal alteration minerals or sulfate and borate-rich evaporite minerals in the field, but we can readily identify many such minerals on the basis of intrinsically unique spectral signatures (Hunt, 1977), many of which occur at wavelengths the human eye is not sensitive to. The parameters in spectra such as absorption feature wavelength, width, asymmetry, and depth help to distinguish between minerals (van der Meer, 2004).

The visible and near infrared (VNIR) and shortwave infrared (SWIR) spectral ranges that span 0.4-2.5 µm are where many diagnostic spectral features are found for mineral groups such as smectites, kaolinites, alunite, carbonates, sulfates, hydroxyls, and hydrates. Hyperspectral sensors have hundreds of narrowly spaced contiguous channels, designed to sample and discriminate among these minerals from aircraft or satellite platforms.

Data

Two HyMap hyperspectral data sets were acquired in Dixie Valley by the HyVista Corp. and provide the basis for our analysis. The HyMap airborne sensor measures solar reflected radiation with 125-126 bands between 0.44 – 2.48 µm. In September of 2010, approximately 1300 km^2 in 12 flightlines, or scenes, were acquired over Fairview and Dixie Valleys. In September 2002, ~400 km^2 of hyperspectral data acquisition occurred in 18 flightlines centered over Dixie Meadows. Atmospherically and geometrically corrected radiance and reflectance data with spatial resolution of ~3m were supplied by HyVista. HyVista also provided preliminary mineral maps for 13 minerals for the 2010 Fairview –Dixie Valley data set.

Methods

We analyzed atmospherically corrected reflectance data using statistically-based and feature-based methods in the image processing and data analysis software, ENVI. First, vegetation, shadows, and water bodies were masked from the data. In the statistical approach, the Minimum Noise Fraction (Boardman et al., 1995) (MNF) is a double principle component transform that separates noise from data. The reduced data were input into Pixel Purity Index algorithm, which identifies unique endmembers in the scene. Endmembers of interest were extracted using the n-Dimensional Visualizer tool, which projects the spectral endmembers in an n-dimensional data cloud in which pixels on the margins of the cloud are most unique. Endmembers are selected from this process to be mapped later, in conjunction with endmembers selected from the feature-based methods below.

Feature-based methods are also used to identify spectra with characteristic features in each scene. Decorrelation stretches (DCS) remove correlation from three input bands and generate a highly saturated color map (Gillespie et al., 1986). Absorption band depth (ABD) calculations (Crowley, 1989) were generated to identify pixels with diagnostic absorption features. To produce the ABD image, several bands around the absorption feature shoulder are summed and divided by summed bands surrounding the minimum as a relative gauge of band strength.

To generate mineral abundance maps, the Mixture Tuned Matched Filter (MTMF) algorithm was used with endmembers identified in both the statistical and feature-driven methods described above. The MTMF statistically maps similar spectra in an unknown background (Boardman et al., 1995). User-defined thresholds generate spectral maps over regions of interest. High thresholds results in high confidence picks. The mineral maps were geocorrected and exported to a geodatabase.

In the field and lab, a portable Analytical Spectral Device (ASD) Field Spec Pro field spectrometer was used to measure high resolution data in 2151 channels over the spectral range 0.35-2.5 µm. Spectral transects in the field and individual sample measurements were acquired. The USGS spectral library was used to compare field and lab spectra to known standards and identify minerals in our samples. X-ray diffraction analysis will be performed during the summer of 2011 on hand-gathered samples to corroborate selected mineral compositions.

Results

HyMap-derived mineral maps for two data sets that cover more than 1700 km^2 in Dixie Valley and Fairview Valley, Nevada were generated to locate hydrothermal-related minerals. Kaolinite, alunite, eugsterite, goethite, and opal were mapped in several locations (fig. 2). In most cases the remote sensing results were supported by the field and lab spectral analyses performed on the field samples, and where this was not the case, mineral maps were revised.

In southwestern quadrant of Fairview Mountains, widespread illite/smectite, and discrete locations of alunite, gypsum and

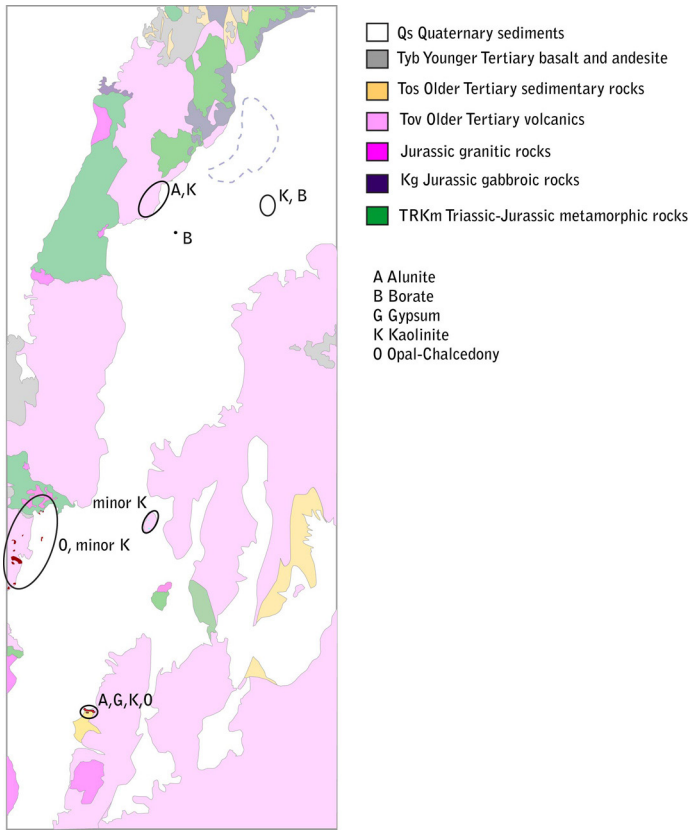

Figure 2. Regional map of remotely sensed hydrothermal minerals in the Fairview Peak-Dixie meadows area. Geological map after Wilden and Speed (1974).

opal-chalcedony, were mapped remotely. This is less than a kilometer west of the Nevada Fairview Mine, where small amounts of silver and gold were mined in the 1930s (Willden and Speed, 1974). The deposit is associated with Tertiary-aged andesite and dacite intruding into Tertiary-aged tuff and volcaniclastic debris (Henry, 1996). In the field we confirmed our mapping results, and also found abundant gypsum, eugsterite, banded chalcedony, and realgar (fig. 3). Many fault damage zones and slickensides were observed in the area, and a small (<3m^2) outcrop of gypsum appears to be forming by the evaporation of groundwater from a seep.

Some of the hydrothermal indicator mineral spectra are not uniquely related to geothermal activity, and can occur in several geological environments. For example, opal-chalcedony was remotely mapped in several locations. The opal described at the location in the previous paragraph is related to hydrothermal alteration, and several other hydrothermal indicator minerals help support this assertion. In La Plata Canyon, our mapping results for opal-chalcedony were associated with silicified Pleistocene lake deposits mapped by Willden and Speed (1974.) Opal-chalcedony also was confirmed in the non-welded zone of Tertiary volcanic tuffs in Sand Springs Mountains. A north-northeast striking lineation on the southeast side of Fairview Mountain was a meters-wide white silicic dike that spectrally mapped as an opal-chalcedony false-positive as a result of spectral ambiguity. Field visits to these locations quickly determined context of the geological environment, and relevance to hydrothermal mineral mapping.

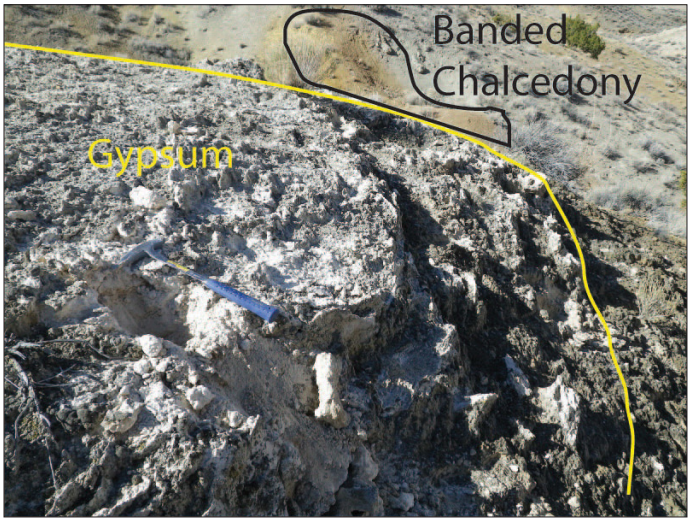

Figure 3. Gypsum mound mapped remotely in southwest Fairview Peak. A thick vein (~5 cm) of banded chalcedony abutted it, and may have been fault controlled.

In the Dixie Meadows area, we confirmed strong argillic alteration that consisted of kaolinite, alunite, and calcite alteration in the range that agrees with previous hyperspectral mineral mapping by Kennedy Bowdoin (2003). Additionally, borates and kaolinite were mapped in the Dixie Lake area in the valley floor. Kainite, a borate, was field verified with the ASD spectrometer, south of Dixie Meadows (fig. 2). Kaolinite and borates were spectrally mapped in the playa east of Dixie Lake over a 12 km^2 area.

Spectrally derived maps of micas were not good indicators of hydrothermal alteration. The spectrally-derived mapped areas were frequently found to be weathering Miocene volcanic deposits (e.g. in the Piroutte Mountain area) or related to intrusives of Miocene or older age (e.g. in the Elevenmile Canyon). Our results suggest the best potential for further exploration is in the Dixie Meadows area and along the southwest side of Fairview Peak.

Field checking the spectra helped to discern false positives. In all cases, the spectral analysis pointed to areas of alteration and interest. Additional field work and sampling will occur in summer 2011 and we will report on the final mapped mineralogy at the meeting in October.

References

Bennett, R. A., B. P. Wernicke, N. A. Niemi, A. M. Friedrich, and J. L. Davis, 2003, Contemporary Strain Rates in the Northern Basin and Range Province from GPS Data: Tectonics, v. 22, p. 31.

Bell, J. W., S. J. Caskey, A. R. Ramelli, and L. Guerrieri, 2004, Pattern and rates of faulting in the Central Nevada Seismic Belt, and paleoseismic evidence for prior beltlike behavior: Bulletin of the Seismological Society of America, v. 94, p. 1229-1254.

Blackwell, D. D., R. P. Smith, and M. C. Richards, 2007, Exploration and development at Dixie Valley, Nevada: summary of DOE studies, 32nd Workshop on Geothermal Reservoir Engineering, Stanford University, Stanford, California.

Boardman, J.W., Kruse, F.A., Green, R.O., 1995. Mapping target signatures via partial unmixing of AVIRIS data, Proceedings of the Fifth JPL Airborne Earth Science Workshop. JPL Publication, pp. 23-26.

Browne, P.R.L., 1978. Hydrothermal alteration in active geothermal fields. Annu. Rev. Earth Planet. Sci. 6, 229-250.

Caskey, S. J., S. G. Wesnousky, P. Shang, and D. B. Slemmons, 1996, Surface faulting of the 1954 Fairview Peak (Ms 7.2) and Dixie Valley (Ms 6.8) earthquakes, Central Nevada: Bulletin of the Seismological Society of America, v. 80, p. 761-787.

Coolbaugh, M., Lechler, P., Sladek, C., Kratt, C., 2010. Lithium in Tufas of the Great Basin: Exploration Implications for Geothermal Energy and Lithium Resources GRC Transactions 34.

Crowley, J.K., Brickey, D.W., Rowan, L.C., 1989. Airborne Imaging Spectrometer Data of the Ruby Mountains, Montana: Mineral Discrimination Using Relative Absorption Band-depth Images. Remote Sensing of the Environment 29, 121-134.

Faulds, J. E., M. F. Coolbaugh, G. S. Vice, and M. E. Edwards, 2006, Characterizing Structural Controls of Geothermal Fields in the Northwestern Great Basin: A Progress Report, v. 30, p. 8.

Gillespie, A. R., Kahle, A. B., and Walker, R. E., (1986). Color Enhancement of HighlyCorrelated Images. I. Decorrelation and HIS Contrast Stretches. Remote Sensing of Environment, v. 20; p. 209-235.

Hammond, W. C., C. Kreemer, and G. Blewitt, 2009, Geodetic constraints on contemporary deformation in the northern Walker lane: 3. Central Nevada seismic belt postseismic relaxation: The Geological Society of America, v. Special Paper 447, p. 33-54.

Henry, C.D., 1996. Geologic Map of the Bell Mountain Quadrangle, western Nevada, Nevada Bureau of Mines and Geology Field Studies Map 12c.

Hunt, G. R., 1977, Spectral signatures of particulate minerals in the visible and near infrared: Geophysics, v. 42, p. 501-513.

John, D.A., 1995. Tilted middle Tertiary ash-flow calderas and subjacent granitic plutons, southern Stillwater Range, Nevada: Cross sections and Oligocene igneous center. GSA Bulletin 107, 180-200.

Kennedy Bowdoin, T., 2003. The Chemical and Structural Dynamics of the Geothermal System at Dixie Meadows, Nevada Using Hyperspectral Imaging and Field Observations, Earth Sciences. University of Santa Cruz, Santa Cruz, p. 103.

Kratt, C., W. Calvin, and M. Coolbaugh, 2006, Geothermal Exploration with Hymap hyperspectral data at Brady-Desert Peak, Nevada: Remote Sensing of the Environment, v. 104, p. 313-324.

Kruse, F. A., J. W. Boardman, and J. F. Huntington, 1999, Fifteen Years of Hyperspectral Data: northern Grapevine Mountains, Nevada: 8th JPL Airborne Earth Science Workshop, p. 247-258.

Mankhemthong, N., Oppliger, G.L., Aslett, Z., 2008. Structural localization of two low temperature geothermal systems within the gravity defined linkage between Dixie Valley and Fairview Valley, Nevada, USA. GRC Transactions 32, 250-254.

Renaut, R.W., Jones, B., Tiercelin, J.-J., Tartis, C., 2002. Sublacustrine Precipitation of Hydrothermal Silica in Rift Lakes: Evidence from Lake Baringo, central Kenya Rift Valley. Sedimentary Geology 148, 235-257.

Reyes, A.G., 1990. Petrology of Phillippine geothermal systems and the application of alteration mineralogy to their assessment. Journal of Volcanology and Geothermal research 43, 279-309.

Rowan, L.C., Hook, S.J., Abrams, M.J., and J.C. Mars, 1998. Mapping hydrothermally altered rocks at Cuprite, Nevada, using the Advanced Spaceborne Thermal Emission and Reflection Radiometer (ASTER), a new satellite-imagining system. Economic Geology, v. 98, p. 1019-1027.

van der Meer, F., 2004. Analysis of spectral absorption features in hyperspectral imagery. International Journal of Applied Earth Observation 5, 55-68.

Vaughan, G. R., S. J. Hook, W. M. Calvin, and J. V. Taranik, 2005, Surface mineral mapping at Steamboat Springs, Nevada, U.S.A., with multi-wavelength thermal infrared images: Remote Sensing of Environment, v. 99, p. 140-158.

Willden, R., Speed, R.C., 1974. Geology and Minerals Deposits of the Churchill County, Bulletin 83. Nevada Bureau of Mines and Geology.